HHS Public Access

Author manuscript

Exp Mol Pathol. Author manuscript; available in PMC 2017 August 17.

Published in final edited form as:

Exp Mol Pathol. 2017 August ; 103(1): 56–70. doi:10.1016/j.yexmp.2017.06.010.

NKG2D ligand expression in Crohn's disease and NKG2D-dependent stimulation of CD8+ T cell migration

Kasper Vadstrup[a,b,c,d,*], **Elisabeth Douglas Galsgaard**[c], **Helle Jensen**[d], **Lewis L. Lanier**[d], **James C. Ryan**[d,e], **Shih-Yu Chen**[f], **Garry P. Nolan**[f], **Marianne Kajbæk Vester-Andersen**[a], **Julie Steen Pedersen**[a], **Jens Gerwien**[c], **Teis Jensen**[c,1], and **Flemming Bendtsen**[a,b]

[a]Gastrounit, Medical Division, Hvidovre University Hospital, DK-2650 Hvidovre, Denmark

[b]Faculty of Health Sciences, The Panum Institute, University of Copenhagen, DK-2200 Copenhagen N, Denmark

[c]Biopharmaceutical Research Unit, Novo Nordisk A/S, DK-2760 Maaloev, Denmark

[d]Department of Microbiology and Immunology, University of California, San Francisco, San Francisco, CA 94143, USA

[e]Department of Medicine, Veterans Affairs Medical Center and University of California San Francisco, San Francisco, CA, USA

[f]Department of Microbiology and Immunology, Stanford University, Stanford, CA 94305, USA

Abstract

Interaction between the activating NKG2D receptor on lymphocytes and its ligands MICA, MICB, and ULBP1–6 modulate T and NK cell activity and may contribute to the pathogenesis of Crohn's disease (CD). NKG2D ligands are generally not expressed on the cell surface of normal, non-stressed cells, but expression of MICA and MICB in CD intestine has been reported. In this exploratory study, we further characterize the expression of NKG2D and its ligands, including the less well-described ULBP4–6, in CD, and test if NKG2D ligand interactions are involved in the migration of activated T cells into the affected mucosal compartments. Intestinal tissue from CD patients and healthy controls were analyzed by flow cytometry, mass cytometry, and immunohistochemistry for expression of NKG2D and ligands, and for cytokine release. Furthermore, NKG2D-dependent chemotaxis of activated $CD8^+$ T cells across a monolayer of ligand-expressing human intestinal endothelial cells was examined. Activated lymphocytes down-regulated NKG2D expression upon accumulation in inflamed CD intestine. NKG2D expression on $CD56^+$ T and γδ T cells from inflamed tissue seemed inversely correlated with CRP levels and cytokine release. B cells, monocytes, mucosal epithelium, and vascular endothelium expressed NKG2D ligands in inflamed CD intestine. The expression of NKG2D ligands was correlated with

*Corresponding author at: Medical Affairs, Immunology, Janssen Pharmaceuticals, Birkerød, Denmark. kvadstru@its.jnj.com (K. Vadstrup).

[1]Currently at Cphbusiness Laboratory and Environment, Hillerød, Denmark.

Disclosures

E.D.G. and J.G. are employed at Novo Nordisk A/S. T.J. was employed at Novo Nordisk A/S at the time of study. L.L.L. and the University of California, San Francisco have licensed intellectual property rights regarding NKG2D for commercial applications, otherwise the authors have nothing else to disclose. The authors have declared that no conflict of interest exists.

cytokine release, but was highly variable between patients. Stimulation of vascular intestinal endothelial cells in vitro induced expression of NKG2D ligands, including MICA/B and ULBP2/6. Blockade of NKG2D on $CD8^+$ T cells inhibited the migration over ligand-expressing endothelial cells. Intestinal induction of NKG2D ligands and ligand-induced down-regulation of NKG2D in CD suggest that the NKG2D-ligand interaction may be involved in both the activation and recruitment of $NKG2D^+$ lymphocytes into the inflamed CD intestine.

Keywords

IBD; MICA; MICB; ULBP

1. Introduction

Crohn's disease (CD), an inflammatory bowel disease (IBD), is an immunologically mediated, debilitating condition resulting from destructive inflammation of the gastrointestinal tract (Gyires et al., 2014; Ko and Auyeung, 2014). The pathogenesis of IBD is incompletely understood, but the immune activating receptor NKG2D has been implicated in some (Ito et al., 2008; Kjellev et al., 2007), but not all, mouse models of colitis (Guerra et al., 2013). In human IBD, the expression and function of NKG2D have not been well characterized, but a recent phase II clinical trial showed that a blocking antibody against NKG2D induced rapid clinical remission of CD in some patients, implicating NKG2D and its ligands in the pathogenesis of CD (Allez et al., 2014). A better understanding of the expression pattern and functional role of NKG2D ligands in CD will help to guide and optimize NKG2D blockade therapy.

NKG2D is an activating receptor constitutively expressed in on human NK, γδ T, MAIT, $CD56^+$ T, and $CD8^+$ T cells (Carapito and Bahram, 2015; Lanier, 2015), which can participate in the recognition of inducible "stressed-self" ligands on the surface of target cells (Champsaur and Lanier, 2010). Activation of NKG2D triggers cellular proliferation, cytokine production, and target cell killing (Upshaw and Leibson, 2006). Eight human ligands for NKG2D have been identified: MHC class I polypeptide-related sequence A (MICA), MICB, and UL16 binding protein (ULBP) 1 through 6 (also designated RAET1E, RAET1G, RAET1H, RAET1I, RAET1L, and RAET1N), all with marked allelic polymorphisms and different binding affinities for NKG2D (Cerwenka and Lanier, 2001; O'Callaghan et al., 2001). Although transcripts are present in some healthy cell types (Schrambach et al., 2007), the ligand proteins are rarely present on the cell surface of healthy cells, but are inducibly expressed by virus infection, tumorigenesis, or by stimuli such as DNA damage, oxidative stress, heat shock, toll-like receptor signaling, or cytokine exposure (Champsaur and Lanier, 2010; Gonzalez et al., 2006; Gonzalez et al., 2008; Raulet et al., 2013). Low MICA expression has been reported on the cell surface of some healthy cell types including epithelial cells in the gut (Eagle et al., 2009; Groh et al., 1996). Increased MICA expression has also been reported in auto-immune diseases such as type 1 diabetes, celiac disease, rheumatoid arthritis, and atherosclerosis, where it is found on vascular endothelial cells (Allegretti et al., 2013; Caillat-Zucman, 2006; Groh et al., 2003; Hue et al., 2004; Lin et al., 2012). Additionally, associations between MICA alleles and

thyroid disease and Addison's disease have been observed, pointing to these factors of innate immunity contributing to the pathogenesis of autoimmune disorders (Bilbao et al., 2003; Cho et al., 2012). Increased levels of MICA and/or MICB have also been observed on epithelial cells and monocytes in CD patients, where they may trigger cytokine release and cytolytic activity (Allez et al., 2007; Glas et al., 2001; La Scaleia et al., 2012; Orchard et al., 2001). Analyses of ULBP1–6 expression in human CD are incomplete, but ULBP1 and ULBP2 expression have been reported on intestinal monocytes from CD patients (La Scaleia et al., 2012).

The aims of the present study are to characterize the relation of NKG2D ligands to Crohn's disease. Multiple methods were applied as ligand expression is regulated on many levels (Lanier, 2015; Raulet et al., 2013). We here use immunohistochemistry (IHC), Cytometry by Time of Flight (CYTOF or mass cytometry), flow cytometry, and RNA analysis to characterize the expression of NKG2D and its ligands in intestinal samples and peripheral blood cells from CD patients and healthy controls. Furthermore, we examined the contribution of NKG2D to the migration of $CD8^+$ T cells over a monolayer of human intestinal microvascular endothelial cells (HIMEC) with in vitro induced expression of NKG2D ligands.

2. Materials & methods

2.1. Patient population

For flow cytometry, RNA analysis, and cytokine quantification of all ligands, the study population was comprised of 6 CD patients referred for surgery, including 4 women and 2 men with a median age of 36 years with an average disease duration of 8 years and a median level of the serum inflammatory marker C-reactive protein (CRP) value of 64 mg/L (range; 0.3–190 mg/L). None of the CD patients were currently receiving IBD medications, but four had previously been on anti-TNF-α treatment (2× three weeks, three years and four years prior to enrollment). Study subjects donated inflamed and uninflamed portions of resected caecum or colon for experimental analyses. Areas from ileum were not included. Six drug-free healthy control subjects with a median age of 49 years and a median CRP 1.5 mg/L donated 8 normal colonic biopsies obtained during endoscopy. They were recruited from a colon cancer screening program and had no symptoms or signs of intestinal disease. All control subjects were above 18 years of age without pregnancy, HIV infection, and without any infections at time of surgery or endoscopy. Blood samples were taken within 14 days of endoscopy or surgery for biochemical analyses of CRP.

For mass cytometry analysis, peripheral blood samples and intestinal biopsies were collected during endoscopy from two patients with Crohn's disease. Patient #1 had a J-pouch performed due to initial suspicion of ulcerative colitis, but the diagnosis was revised to CD after histological analysis of the colectomy specimen was finalized. Biopsies were taken from the ileum, as well as inflamed and non-inflamed areas of the ileal J-pouch. Patient #2 had a normal colon and an inflamed ileum with a low-grade non-ulcerated stricture. Biopsies were taken of the normal colon and the inflamed ileal stricture. On the same day as the biopsies, peripheral blood samples were collected in EDTA tubes.

For histology analyses, additional intestinal tissue samples from CD patients (total n = 17) and normal controls (n = 10) were included. The latter samples originated from patients undergoing intestinal surgery due adenocarcinoma and were histologically within normal range. CD and normal control samples were sourced from Asterand UK Ltd. and diagnoses were confirmed by Dr. Lene Buhl Riis, Consultant, Specialist in Pathology, Herlev Hospital, Denmark. For use as positive control tissues, tonsil tissue samples were collected from patients that had their tonsils surgically removed due to tonsillitis at the Copenhagen University Hospital and Gentofte Hospital in Denmark.

2.2. Immunofluorescence

Acetone-fixed cryosections were stained as described above. Mouse anti-human NKG2D antibody (2 μg/ml, clone 149,810/MAB139, R & D Systems) together with either rabbit anti-CD3 (clone SP7, Neomarkers, Fremont, CA, USA) or rabbit anti-CD8 (clone SP16, Spring Bioscience, Pleasanton, CA, USA) antibodies were applied overnight at 4 °C. Anti-NKG2D antibody was detected by Vectastain and biotinylated TSA, followed by Alexa-488 conjugated streptavidin (Invitrogen), whereas anti-CD3 and -CD8 were detected by Alexa-594 conjugated anti-rabbit IgG secondary antibodies (Jackson ImmunoResearch). Nuclei were counterstained with Hoechst dye. Sections were mounted in Fluorescent Mounting Medium (DAKO). The protocol was validated on samples from human tonsils (Suppl. Fig. 1). The frequency of $NKG2D^+$ cells in intestinal samples was semi-quantitatively evaluated on anti-NKG2D and anti-CD8 double immunofluorescence-stained cryosections using microscopy (Zeiss epi-fluorescence microscope: Axio Imager M2, Oberkochen, Germany). Score 0: no NKG2D-positive cells, Score 1+: a few scattered positive cells as observed in normal mucosa, Score 2+: moderate mucosal infiltration of positive cells as observed in some CD samples, and Score 3+: numerous positive cells as observed in lymphoid aggregates. The percentage of $NKG2D^+$ or $CD8^+$ cells was calculated based on counting single- and double-positive cells that were identified on 40× images (3 representative and randomly selected images per tissue section) taken with a Axio Cam MRm camera on a Axio Imager M2 using the Zen2012 software.

2.3. Flow cytometry analysis

Cells isolated from the inflamed CD resection tissues were analyzed by flow cytometry. After stripping of the muscular layers, the upper part of the tissue was incubated twice, while stirring, for 30 min in 20 ml HBSS containing penicillin, streptomycin, and 1 mM EDTA (Gibco) to remove the epithelial layer and prepare an epithelial cell population. The remaining tissue was cut into very fine pieces using forceps and surgical scalpels. The minced tissue was incubated with freshly prepared collagenase II (0.5 mg/ml) and 10 U/ml DNase I (Sigma-Aldrich) three times for 30 min with slow rotation. The supernatant containing lamina propria cells (LPC) was filtered through a 70 μm cell strainer (Falcon) and washed twice with RPMI-1640 with 10% FCS and 1% penicillin and streptomycin (Gibco) to obtain a LPC population. Two flow cytometry panels of fluorochrome-labeled anti-human monoclonal antibodies were used to analyze NKG2D receptor and ligand expression on the isolated LPC (Suppl. Table 1). Panel 1 consisted of: BV421-conjugated anti-CD56, PerCP-Cy5.5-conjugated anti-CD3, APC-conjugated anti-NKp46, FITC-conjugated anti-CD45, AF700-conjugated anti-CD8, BV605-conjugated anti-CD4 (BD Bioscience, San Jose, CA,

USA), and PE-conjugated anti-NKG2D (eBioscience, San Diego, CA, USA). Panel 2 consisted of: PerCP-Cy5.5-conjugated anti-CD3, BV605-conjugated anti-CD4, AF700-conjugated anti-CD14, BV421-conjugated anti-CD11c, FITC-conjugated anti-CD45, BV650-conjugated anti-CD19, PE-Cy7-conjugated anti-CD31 (BD Bioscience), and APC-conjugated anti-CD326 (EPCAM) (eBioscience). In addition, unconjugated monoclonal antibodies against the following NKG2D ligands were included in panel 2: MICA, MICB, ULBP1, ULBP2, ULBP3 (BamOmaB, Gräfelfing, Germany), ULBP4, ULBP5, and ULBP6 (Novo Nordisk, Beijing, China). One million LPC were stained with only FITC-conjugated anti-CD45, all antibodies in panel 1 except PE-conjugated anti-NKG2D, or Fluorescence Minus One (FMO) control including isotype-matched control staining. Panel 2 or FMO control was applied to both the epithelial cell and LPC populations. Cells were incubated with the anti-NKG2D ligand antibodies, followed by PE-conjugated-polyclonal goat anti-mouse IgG antisera (Jackson ImmunoResearch, West Grove, PA). Finally, the cells were incubated with LIVE/DEAD® Fixable Violet Dead Cell Stain (Invitrogen, Waltham, MA, USA), and analyzed on a LSR Fortessa (BD Bioscience) using Kaluza software (Beckman Coulter, Brea, CA). The specific reactivity and titration of the anti-NKG2D ligand antibodies obtained from BAMOMAB and Novo Nordisk were determined on HEK cells transiently transfected with cDNA plasmids encoding the NKG2D ligands (Novo Nordisk).

2.4. Mass cytometry

Biopsies were collected in RPMI-1640 containing 15% FBS (Thermo Scientific, Waltham, MA, USA), 2 mM L-glutamine (UCSF cell culture facility), penicillin (100 IU), and streptomycin (100 μg/ml) (Corning Cellgro) (designated R-15 medium). Single cells were isolated from the intestinal biopsies using collagenase type II as previously described (Shacklett et al., 2003) with minor modifications. Briefly, the intestinal biopsies were washed once in R-15 medium, and then incubated in collagenase type II and DNase I solution (0.5 mg/ml collagenase type II) (Worthington Biochemical Corporation, Lakewood, NJ, USA) and 0.1 mg/ml DNase I (Roche Diagnostics, Risch-Rotkreuz, Switzerland) in RPMI-1640 medium containing 7.5% FBS, L-glutamine, penicillin and streptomycin for 30 min at 37 °C with intermittent rotation. The biopsies were further disrupted by forcing the suspension through a 16-gauge needle (BD Biosciences) and the entire suspension was passed through a 70 μm cell strainer (Fisher Scientific). The cells were immediately washed twice in R-15 medium containing 0.1 mg/ml DNase 1. The 30 min collagenase incubation, needle disruption, and wash procedure was repeated two or three times for the remaining tissue fragments. PBMCs were isolated from blood samples by density gradient centrifugation using Ficoll-Paque™ PLUS (GE Healthcare BioSciences, Staffanstorp, Sweden). In each case, cells isolated from blood and biopsies were processed and analyzed on the day of isolation. Labeling of cells and viability staining for mass cytometry was performed as previously described (Bendall et al., 2011; Fienberg et al., 2012) with minor modifications. Briefly, viability stain was done by incubating the cells with 50 μM cisplatin (Sigma-Aldrich) in 1 ml serum-free RPMI-1640 medium/10^6 cells for 1 min at room temperature (RT). An equal volume of RPMI-1640 medium containing 10% FBS, L-glutamine, penicillin, and streptomycin (R-10 medium) was added and then the cells were incubated for an additional 5 min at RT. The cells were washed in cell staining media (CSM: Phosphate-buffered saline (PBS) with 0.5% bovine serum albumin (BSA) and 0.02% sodium

azide) and surface stained by incubating with a cocktail of metal-conjugated antibodies as listed in Suppl. Table 2 for 1 h at RT with continuous shaking. Cells were washed twice with CSM, fixed with 1.5% paraformaldehyde (PFA) in PBS for 10 min at RT, and permeabilized in cold methanol for 10 min at 4 °C. Intracellular staining was performed by incubating the cells with ^{173}Yb-conjugated anti-cPARP antibody for 1 h at RT with continuous shaking. Cells were washed twice with CSM and then incubated for 20 min in 1 ml of Iridium DNA intercalator (diluted 1:5000 in PBS with 1.6% PFA; DVS Sciences, San Francisco, CA, USA) for 20 min at RT or overnight at 4 °C. Prior to mass cytometry analysis, cells were washed once with CSM, twice with double-distilled water, and then re-suspended in double-distilled water containing the bead standard for normalization (Finck et al., 2013). Cells were resuspended in double-distilled water at approximately 1×10^6 cells per ml and analyzed on a CyTOF™ mass cytometer (Fluidigm).

2.5. Ex vivo cytokine quantification

Biopsies and resections were transported on ice in Dulbecco's Modified Eagle Medium (DMEM) liquid (High Glucose) with GlutaMAX™ I (Gibco, Grand Island, NY) and processed within 1 h. CD biopsies were pinched from the visibly inflamed parts, determined by the surgeon. Part of the tissue was stripped of the muscular layers with scalpels, and 3 mm biopsies were punched out from the upper mucosal layer (Miltex, York, PA). Intestinal biopsies were cultured ex vivo as previously described with minor modifications (Browning and Trier, 1969; Tsilingiri et al., 2012). In brief, biopsies were incubated for 24 h on specially constructed steel grids in an airtight chamber filled with a carbogen mixture of 95% O_2 and 5% CO_2. The culture medium was composed of 1 ml DMEM with GlutaMAX™ I supplemented with 10% fetal bovine serum (FBS), 1% non-essential amino acids, 1% sodium pyruvate, 1% penicillin and streptomycin (all Gibco), 50 mg/ml gentamicin, and 10 μg/ml insulin-transferrin-selenium-X (Sigma-Aldrich, St. Louis, MO). The medium was dispensed into a center-well organ culture dish (Falcon, Corning, Tewksbury, MA). Biopsies were carefully placed with an apical to basolateral polarity on the T-disk with the latter side in contact with the medium below. Secretion of IL-1β, IL-10, GM-CSF, IFN-γ, and TNF-α was measured in the conditioned medium by Bio-plex Pro Technology on a Bio-plex 200 multiplex system (Biorad, Hercules, CA), according to the manufacturer's instructions. All values were normalized to weight of the biopsies and given as pg/ml/100 mg tissue.

2.6. Immunohistochemistry

Cultured cells and tissue samples were embedded in Tissue Tek® O.C.T Compound (Sakura, Alphen aan den Rijn, The Netherlands) and snap-frozen. Sections (5 μm) were fixed in acetone (−20 °C) for 10 min and air-dried. Unless otherwise indicated, all following steps were performed at RT and the sections were washed in Tris-buffered saline (TBS) with 0.01% Tween20 (BDH, London, UK) between each step. Endogenous peroxidase activity was blocked by Dual Block (DAKO, Glostrup, Denmark) and endogenous biotin was blocked by Biotin Blocking System (Invitrogen). Non-specific binding of antibodies was blocked by pre-incubation in TBS with 3% human serum (Jackson ImmunoResearch), 7% donkey serum (Jackson ImmunoResearch), 3% bovine serum albumin (BSA) fraction V (Hyclone), and 3% non-fat dry milk (DIFCO). Anti-MICA/B BAMO1 (0.33 μg/ml) and

anti-MICA AMO1 (1 μg/ml) monoclonal mouse antibodies (BamOmaB) or isotype-matched control IgG1 (1 μg/ml, R & D Systems, Minneapolis, MN, USA) were diluted in the TBS buffer used for blocking and applied overnight at 4 °C. Biotinylated donkey anti-mouse IgG1 secondary antibody (0.17 μg/ml, Jackson ImmunoResearch) was added followed by avidin-biotin-horse radish peroxidase complexes (Vectastain, Vector Labs, Burlingame, CA, USA), biotinylated tyramide (Tyramide signal amplification (TSA) kit, NEL700, Perkin Elmer, Waltham, MA, USA), and Vectastain. Antibody binding was visualized by diaminobenzidine (DAB) and nuclei were counterstained with hematoxylin. Sections were mounted in Pertex and then analyzed by microscopy. Mouse Ba/F3 cells stably transfected with MICA*0019, (CT7 MICA cells) or mouse P815 cells stably transfected with MICB*002 (CT461 MICB cells) were used as positive controls to validate the antibody reactivity (Suppl. Fig. 2). Negative controls were parental Ba/F3 and P815 cells, respectively. As shown in Suppl. Fig. 2 the anti-MICA antibody AMO1 strongly stained cryo-sections of MICA-transfected cells. This antibody did not cross-react with the closely related MICB protein. In contrast, the anti-MICA/B antibody BAMO1 recognized both MICA- and MICB-transfected cells, demonstrating that the two antibodies react with two different epi-topes. Both antibodies failed to stain the parental Ba/F3 and P815 cells. Isotype-matched control immunoglobulins were used as controls for specific staining.

2.7. mRNA analysis by qPCR

Inflamed pinch biopsies from 6 CD patients and normal biopsies from 6 healthy controls were sent in RNA stabilization solution RNAlater® (Ambion, Life Technologies, Carlsbad, CA) to AROSAB (Aarhus, Denmark) for mRNA analysis. RNA was extracted from the biopsy tissue that had been cultured overnight to quantify cytokine release in the explant assay. An Applied Biosystems 7900HT platform was used to perform qPCR experiments with TaqMan reactions (Thermo Fisher Scientific, Waltham, MA). Transcripts were analyzed with TaqMan probes for KLRK1 (NKG2D), MICA, MICB, ULBP1, ULBP2, ULBP3, ULBP4, ULBP5, and ULBP6.

2.8. Migration assay

Human intestinal microvascular endothelial cells (HIMEC) were isolated as previously described from surgically resected (non-IBD) colonic specimens at The Cleveland Clinic (Cleveland, OH, USA) (Binion et al., 1997) and shipped in culture overnight. HIMEC were cultivated as directed (Rieder et al., 2011) and used between passage 8 and 11. Human large intestine microvascular endothelial cells (HLIMEC) established from normal human large intestine (colon) tissue were purchased from Cell Systems (Kirkland, WA, USA). The cells were grown and passaged in CSC Complete Medium according to manufacturer's instructions (Cell Systems). HLIMEC were used between passage 7 and 9. HIMEC and HLIMEC were primary cells and stimulated at confluence in 24-well plates with 100 U/ml human IFN-α (Sigma-Aldrich) and 1 μg/ml lipopolysaccharide (LPS, Sigma-Aldrich) for 10 h and analyzed for NKG2D ligand expression as described above. $CD8^+$ T cells were isolated from buffy coats from anonymous blood donors by Ficoll-Hypaque (Sigma-Aldrich) centrifugation and by subsequent negative selection (EasySep, Stemcell Technologies, Grenoble, France). The cells were stimulated with 10 μg/ml plate-bound anti-CD3 antibodies (SK7, eBioscience) and 200 U/ml IL-2 (Sigma-Aldrich) in non-treated

polystyrene, standard tissue culture 96-well plates (Falcon, Corning) for three days and then incubated with IL-2 only for another 9 days in 6-well plates (Corning) to generate cells that were responsive to NKG2D stimulation. NKG2D-responsiveness was confirmed by re-stimulating the cells with plate-bound 10 μg/ml anti-CD3 and 5 μg/ml anti-NKG2D antibodies (BioLegend, San Diego, CA, USA) or isotype-matched control Ig (10 μg/ml) in 96-well plates as above for 4 h and then analyzed for intracellular IFN-γ (BioLegend) and CD107a (BioLegend) expression by flow cytometry. Migration assays were performed using 5.0 μm transwell plates (Corning) with a confluent monolayer of HLIMEC and 500,000 activated (as described above) $CD8^+$ T cells in the top chamber, and incubated with or without 10 μg/ml blocking anti-NKG2D antibody or isotype-matched control Ig (low endotoxin and azide free, BioLegend). The migration through the endothelial layer in response to 100 ng/ml CXCL10 (BioLegend) was examined over 4 h and quantified by cell counting using flow cytometry analysis. Expression of the CXCL10 receptor, CXCR3, and NKG2D on $CD8^+$ T cells was confirmed beforehand by flow cytometry. Samples without HLIMEC or with CXCL10 in the top chamber were included as negative controls.

2.9. Statistics

Flow cytometry: One-Way ANOVA was used to test differences in cell specific expression of NKG2D. Linear regression was used to test correlations, with $P < 0.05$ meaning that the slope is significantly nonzero. *IHC*: the frequency of $NKG2D^+$ cells (i.e. score) and the percentage of $NKG2D^+CD8^+$ cells of $NKG2D^+$ or $CD8^+$ cells, respectively, are expressed as mean ± standard deviation and analyzed by Kruskal-Wallis test with multiple comparisons. *qPCR and migration*: unpaired *t*-test of the means comparing gene expression in CD vs. normal control, and migrating cell number. Differences were considered statistically significant when $P < 0.05$.

2.10. Study approval

The patients for flow cytometry, qPCR and cytokine release studies were recruited at the Amager and Hvidovre Hospitals in Denmark, after signing written consent under the ethical protocol H-1-2012-137 approved by The Danish National Committee for Health Research Ethics.

The patients for mass cytometry were recruited after signing informed written consent under protocols approved by the Institutional Research Boards of the University of California and the Veterans Affairs Medical Center in San Francisco (Human Research Protection Program protocol 12-09140) in accordance with internationally accepted research guidelines.

For histology analyses, tissue from CD patients and normal controls were obtained from Cytomyx/Origene (Cambridge Bioscience, UK). These samples were collected with informed consent. Tissue collection was approved by local bioethics committees. Tonsil tissue samples were collected with informed consent at the Copenhagen University Hospital and Gentofte Hospital in Denmark. The study was approved by the local bioethics committee (protocol no. 1005410 and H-KF-2007-0048).

All authors had access to the study data and had reviewed and approved the final manuscript.

3. Results

3.1. Diverse NKG2D surface expression is detected on lymphocyte populations from CD and normal intestine and at inflamed and non-inflamed sites

We examined the NKG2D expression on lymphocytes in CD and normal intestine by immunofluorescence microscopy. In patients with CD, NKG2D$^+$ cells accumulated in lymphoid aggregates throughout the intestinal wall, whereas in normal intestine, NKG2D$^+$ cells were identified as scattered lamina propria mononuclear cells (LPMC) (Fig. 1A) and intraepithelial lymphocytes (IEL) (data not shown). Moreover, NKG2D$^+$ cells localized to the T-cell zone of isolated lymphoid follicles (Suppl. Fig. 3). When quantitatively scored, the frequency of NKG2D$^+$ cells was significantly increased in CD patients compared to normal controls, presumably due to the increased numbers of lymphoid aggregates (Fig. 1B, Suppl. Fig. 4). Co-staining showed that CD8$^+$ lymphocytes constituted the majority (> 90%) of NKG2D$^+$ cells (Fig. 1A, Suppl. Fig. 4). Moreover, immunofluorescence showed that a high frequency of CD8$^+$ T cells expressed NKG2D in CD (Fig. 1C) by both flow cytometry (88 ± 13%) and mass cytometry (Fig. 1E, F and G). Gating examples are provided in Fig. 1D. Additionally, flow cytometry showed a high frequency of γδ T cells expressing NKG2D (73 ± 10%), with lower frequencies of CD56$^+$ T cells (γδ TCR$^-$), NK cells, and CD4$^+$ T cells expressing NKG2D (31 ± 8.3%, 58 ± 10%, 8 ± 2.5%, respectively); (Fig. 1E). Similar relative differences in the frequency of NKG2D$^+$ cells were observed by mass cytometry (Fig. 1F). In contrast to data obtained by immunofluorescence, no difference in NKG2D expression could be detected between CD patients and normal controls when analyzed at the mRNA level by qPCR (Suppl. Fig. 5). Furthermore, a tendency towards a lower percentage of NKG2D$^+$ CD8$^+$ T cells was observed in CD intestine compared to normal controls as determined by immunofluorescence (Fig. 1C). Similarly, nearly all lymphocyte populations showed lower frequency of cells expressing NKG2D in intestine versus peripheral blood, as well as in inflamed versus non-inflamed sites of CD intestine using mass cytometry (Fig. 1F + G). The opposite expression pattern was observed for the activation marker CD69, which has been suggested to reflect immune responses at mucosal sites (Radulovic and Niess, 2015). A high frequency of lymphocytes isolated from inflamed and non-inflamed sites of CD intestine displayed CD69 expression, whereas no or low expression was observed on lymphocytes isolated from peripheral blood (Fig. 1H). This confirms that the isolated cells were activated at mucosal sites.

3.2. The frequency of γδ and CD56$^+$ T cells expressing NKG2D correlate oppositely with the degree of inflammation in CD patients

In contrast to CD8$^+$ and CD4$^+$ T cells, which showed consistently a high or low frequency of cells expressing NKG2D, respectively, the frequency of NK, γδ T, and CD56$^+$ T cells expressing NKG2D was highly variable between the six CD patients examined (one-way ANOVA analysis, $P = 0.0042$, Fig. 1H). To test if the heterogeneity in frequency of NK, γδ T, and CD56$^+$ T cells expressing NKG2D could be explained by differences in inflammation between the six CD patients, we used linear regression to correlate the frequency of cells expressing NKG2D and amounts of the inflammatory marker C-reactive protein (CRP) in the sera (Fig. 2A). CRP levels correlated negatively with the frequency of CD56$^+$ T cells expressing and positively with frequency of γδ T cells expressing NKG2D ($R^2 = 0.73$ and

0.81, respectively, $P < 0.05$). No correlation was seen for NK, $CD4^+$ T, and $CD8^+$ T cells ($P > 0.05$ for regression line to be non-zero, Fig. 2A and data not shown). In addition, we measured cytokine release from the resection material cultured ex vivo for 24 h in an explant assay. The pro-inflammatory cytokines GM-CSF, IL-1β, IFN-γ, and TNF-α tended to correlate positively with CRP levels, whereas the anti-inflammatory cytokine IL-10 tended to correlate negatively with CRP levels (Fig. 2B). When cytokine release was correlated with the frequency of cells expressing NKG2D, the frequency of $NKG2D^+$ γδ T cells correlated positively with the release of IL-10 and negatively with the release of pro-inflammatory cytokines in the explant assay with GM-CSF being significant (Fig. 2C). The opposite was observed for $CD56^+$ ($\gamma\delta^-$) T cells (Fig. 2D).

3.3. MICA and MICB protein expression is induced in inflamed CD intestine

The tendency towards a lower frequency of lymphocytes expressing NKG2D isolated from inflamed CD intestine (Fig. 1) could be a result of interaction with NKG2D ligands, which is known to cause down-modulation of the receptor (Chalupny et al., 2006; Jimenez-Perez et al., 2012). We, therefore, examined the expression NKG2D ligands on both lymphocytes and tissue cells isolated from CD patient samples by immunohistochemistry, flow cytometry, mass cytometry, and qPCR. The overall mRNA level of MICA and MICB was similar between tissue samples from CD patients and healthy controls (Suppl. Fig. 5). However, mass cytometry data showed that B cells and $CD4^+$ T cells isolated from inflamed CD intestine expressed cell surface MICA at a markedly higher frequency compared to cells isolated from non-inflamed CD intestine or from peripheral blood (Fig. 3A). Although these data suggest an induction of MICA expression on these subsets, the overall frequency of $MICA^+$ B and $CD4^+$ T cells remained low in inflamed CD intestine. This was confirmed by flow cytometry, which showed MICA expression on 5 ± 3% and 1 ± 0.6% on B cells and $CD4^+$ T cells, respectively (Fig. 3B and C). In addition, MICA was detected on $CD14^+$ monocytes/macrophages in inflamed CD intestine by flow cytometry (4 ± 2%; Fig. 3C). Flow cytometry also revealed MICB expression at similar frequencies on B cells and $CD4^+$ T cells and at slightly higher frequencies on monocytes (15 ± 10%) (Fig. 3C). Among the six CD patients, the cell types with the highest frequency of MICA or MIBC positive cells were not always in the same patients (Fig. 3C). IHC analyses of MICA and MICB were performed using two antibodies; BAMO1 recognizing both MICA and MICB and AMO1 recognizing only MICA (Suppl. Fig. 2). Immunostaining for MICA and MICB was observed in the central part of lymphoid aggregates localized in inflamed CD intestine (Fig. 3D). Moreover, MICA and MICB protein expression was observed in granulomas localized in the inflamed CD intestine by IHC (Fig. 3E). Although granulomas strongly suggest Crohn's disease as the diagnosis, they are seen in only ~10% of patients with Crohn's disease and are sporadically distributed in biopsy specimens. Accordingly, we observed granulomas in histological tissue sections from 3 of the 19 patients in the present study. The observed MICA and MICB staining was not localized to cells in the central epithelioid macrophages (Fig. 3E) although, again formal co-localization studies would be required to definitively identify the MICA and $MICB^+$ cell subset(s) within granulomas. Interestingly, the accumulation of $NKG2D^+$ $CD8^+$ cells was observed in both lymphoid aggregates and granulomas (Fig. 3D and E). MICA and MICB immunostaining was also observed in a pattern consistent with that of lymphoid follicle germinal centers. Immunofluorescence

studies with markers of germinal centers would be required to more thoroughly characterize these MICA$^+$ and MICB$^+$ cell subsets. MICA and MICB staining of germinal center-like structures were not unique to CD intestine, but was also observed in normal intestine and tonsil (Suppl. Figs. 6 and 7). Together, these data demonstrate that MICA and MICB proteins are expressed on discrete subsets of immune cells in the inflamed CD intestine.

MICA and MICB protein was expressed not only by intestinal immune cells, but also by non-immune cells (Fig. 4). By IHC, MICA and MICB expression was detected on microvascular endothelial cells in inflamed areas of CD intestine, but not in uninflamed CD intestine or normal control intestine (Fig. 4A). A small subset of CD45$^-$CD31$^+$ endothelial cells in the inflamed CD intestine expressed cell surface MICA (3.1 ± 1.5%) and MICB (2.9 ± 1.8%) when analyzed by flow cytometry (Fig. 4B and C). Note that low numbers of endothelial cells isolated from some samples made the gating sensitive. Similarly, a small subset of CD45$^-$CD326$^+$ mucosal epithelial cells expressed MICA (1.6 ± 0.4%) and MICB (1.8 ± 0.6%) (Fig. 4C). Unfortunately, low level staining was observed with isotype-matched control antibody in mucosal epithelium by IHC (Fig. 4A). Similar staining was observed also when primary antibody was omitted (data not shown) and thus may have been mediated by the tyramide signal amplification detection system. This non-specific staining prevented a definitive quantification of the increased levels of MICA and MICB expression in these cells. Nonetheless, MICA and MICB immunostaining was observed on both epithelial and endothelial cells in tonsils from patients with tonsillitis (Suppl. Fig. 6). Mass cytometry analysis suggested that CD45$^-$ HLA-DR$^+$ cells, which are found within the lymphocyte population (Fais et al., 1987), expressed cell surface MICA to a higher degree than CD45$^-$ HLA-DR$^-$ cells (Fig. 4D). Together these data indicate that MICA and MICB protein expression is induced in epithelial and endothelial cells that co-localize with lymphocytes in inflamed tissues.

3.4. Constitutive expression of MICA and MICB protein in intestinal nervous system

Immunohistochemistry demonstrated MICA and MICB expression on structures morphologically similar to nerve fibers and plexuses. MICA and MICB expressing nerve-like cells were observed throughout the intestinal wall, including mucosal and submucosal nerve fibers (Fig. 4A), as well as myenteric plexuses in the muscular layer (Fig. 3D and Suppl. Fig. 8). The intestinal nervous system appeared to express MICA and MICB constitutively as positive staining of these structures was observed in control intestine as well as in in active and inactive CD.

3.5. ULBP1–6 are expressed at variable levels in inflamed CD intestine across patients

To further characterize the expression pattern of NKG2D ligands in CD intestine we included ULBP1–6 in our mRNA and flow cytometry analyses. The overall mRNA levels were significantly different for ULBP1, 2, and 5, with higher levels observed in whole tissue samples isolated from CD patients compared to healthy controls ($P < 0.05$, *t*-test). The three other ULBP ligands, ULBP3, 4, and 6, showed similar mRNA levels in tissue samples from CD patients and healthy controls (Suppl. Fig. 5).

When ULBP1–6 protein expression was examined by flow cytometry, NKG2D ligands were detected on the surface of both immune cells and resident cells isolated from inflamed areas of CD resection material (Fig. 5A–C). Similar to MICA and MICB, the mean frequencies of ULBP1–6 expressing cells were comparable in $CD14^+$ monocytes (7.2 ± 1.5%), $CD19^+$ B cells (3.6 ± 0.3%), and $CD45^-CD31^+$ endothelial cells (4.5 ± 0.6%), whereas fewer $CD4^+$ T cells and $CD326^+$ epithelial cells expressed ULBP1–6 (1.6 ± 0.2% and 1.7 ± 0.1%, respectively). The patients included in this study exhibited diverse ULBP1–6 expression patterns with only one to two patients expressing high frequencies of ULBP-positive cells (> 10% of a given cell subset) (Fig. 5B and C).

3.6. NKG2D ligand expression and cytokine release

A correlation between NKG2D receptor-ligand expression and cytokine release from the explant assay was examined by linear regression. For $CD19^+$ B cells, there was a significant positive correlation between the frequency of cells expressing MICA/B and the specific release of IL-1β and TNF-α (Fig. 6A, all regression lines have $P < 0.05$, R^2 in figure legend). This positive correlation was strongly influenced by the high frequency of NKG2D ligand expressing cells in one of our six CD patients. MICB, but not MICA, expression on epithelial cells correlated positively with IL-10 release (Fig. 6B and data not shown). There was no significant correlation between cytokine release and MICA and MICB expression on $CD4^+$ T cells, endothelial cells, or monocytes (data not shown). The mean frequency of $ULBP2^+$ cells on a combined group of cellular subsets (monocytes, $CD4^+$ T, $CD19^+$ B, endothelial and epithelial cells) correlated positively with IL-1β and TNF-α release (Fig. 6C). This was true for all the ligands except ULBP1 (data not shown). The ULBP1–6 expression, but not MICA and MICB expression, on monocytes correlated positively with TNF-α release and IL-1β (Fig. 6D and data not shown). ULBP expression on $CD4^+$ T cells correlated positively with IL-10 release (data not shown). In addition, ULBP expression on B cells significantly correlated positively with TNF-α release (data not shown, but similar to Fig. 6A). No significant correlations were observed between NKG2D ligand expression on $CD31^+$ endothelial cells and cytokine release (data not shown).

3.7. Inducible NKG2D ligands on human intestinal microvascular endothelial cells can augment the migration of $NKG2D^+$ $CD8^+$ T cells

Two types of human intestinal microvascular endothelial cells, human intestinal microvascular endothelial cells (HIMECs) and human large intestine microvascular endothelial cells (HLIMECs) were used to examine the functional effect of NKG2D-ligand expression on lymphocyte migration. A NKG2D-dependent migration mechanism has previously been described (Markiewicz et al., 2012). Unstimulated HIMECs were negative for NKG2D ligand expression when cultured to confluence. After stimulation with LPS and TNF-α or IFN-γ, the expression of NKG2D ligands was induced on the HIMECs, but the morphology of the cells was simultaneously disrupted (data not shown). In contrast, LPS and IFN-α stimulation preserved the morphology of the HIMECs and induced a high level of NKG2D ligands on the cell surface (Fig. 7A and Table 1). Higher frequencies of HIMECs expressed MICA and MICB (98 and 86%, respectively) compared with ULBP (3 to 34% for ULBP1, 3, 4 and 5 and 82% for ULBP2/6) (Fig. 7A). In contrast to HIMECs, HLIMECs showed a high endogenous expression of NKG2D ligands, which was only modestly

increased by LPS and IFN-α stimulation (Table 1). Confluent HIMEC and HLIMEC had similar morphology and expressed similar levels of CD31. These results show that an inflammatory stimulus can induce NKG2D ligand expression on human intestinal microvascular endothelial cells.

For the migration assay we used unstimulated HLIMEC cells, as they were constitutively positive for numerous NKG2D ligands. $CD8^+$ T cells isolated from healthy human blood donors were expanded by anti-CD3 stimulation (3 days) and IL-2 culture for a total of 12 days, as these cells responded to NKG2D-mediated co-stimulation. The NKG2D responsiveness was confirmed by re-stimulating the $CD8^+$ T cells with anti-CD3 or anti-CD3 + anti-NKG2D, where NKG2D potentiated anti-CD3-induced cellular activation as shown by staining for CD107a surface expression (degranulation marker) and intracellular IFN-γ production (Fig. 7B). Cells are thus not anergic. Freshly isolated naïve $CD8^+$ T cells did not respond to NKG2D stimulation (data not shown). The expanded $CD8^+$ T cells expressed both CXCR3 (100%) and NKG2D (84%) (Fig. 7B). The migration assay with HLIMEC and expanded $CD8^+$ T cells in response to CXCL10 revealed a significant inhibition of migration (47% reduction) over the endothelium layer when a blocking anti-NKG2D antibody was included compared to isotype-matched control antibody ($P = 0.0085$, n = 12 transwells from 2 blood donors, Fig. 7C). The control assays with chemokine in the upper and lower transwells or without HIMEC showed equal migration regardless of NKG2D blocking. Together, these results suggest that NKG2D ligand expression on human intestinal microvascular endothelial cells can augment the migration of $NKG2D^+$ $CD8^+$ T cells.

4. Discussion

Our results suggest that NKG2D ligands may participate in the activation and the recruitment of $NKG2D^+$ lymphocytes into the inflamed CD intestine. Moreover, our findings suggest that the inflamed CD intestine is associated with the presence of NKG2D ligands on specific leukocyte subsets and on non-immune (resident) cells, with NKG2D down-regulation on selected lymphocyte subsets. These expression patterns were correlated with the inflammatory status within CD tissue. The presence of activation CD69 confirms that these down-regulations happen at mucosal sites (Radulovic and Niess, 2015). NKG2D was uniformly expressed on most $CD8^+$ T cells but only expressed by a few $CD4^+$ T cells across the six inflamed CD patient samples. In contrast, we observed heterogeneity in NKG2D expression on NK, $CD56^+$ T (defined as $CD45^+CD3^+CD56^+$ γδTCR^-) and γδ T cells (defined as $CD45^+CD3^+$ γδTCR^+). The observed differences in the NKG2D expression might be caused by ligand-induced internalization or due to differences in cytokines in the mucosal gut tissue, as several cytokines are known to either increase (Maasho et al., 2005; Park et al., 2011; Roberts et al., 2001; Zhang et al., 2008) or decrease (Burgess et al., 2006; Castriconi et al., 2003; Crane et al., 2010; Lee et al., 2004; Muntasell et al., 2010) NKG2D on lymphocytes. $CD56^+$ αβT and γδ T cells have previously been found to express NKG2D differently (Jamieson et al., 2002) and the balance between these two cell types might be a modulating factor between self-tolerance and autoimmunity (Liu and Huber, 2011). We found that the frequency of $CD56^+$ T cells was positively correlated with the clinical inflammatory state as measured by circulating CRP levels, and with the

release of pro-inflammatory cytokines GM-CSF, IFN-γ, and TNF-α from cultured biopsies isolated from the same CD patients. The opposite results were observed with γδ T cells. Together these data indicate that NKG2D on $CD56^+$ T and γδ T cells may play different roles in CD. Notably, γδ T cells constitute ~40% of the intraepithelial lymphocytes (Kagnoff, 1998; Lundqvist et al., 1992), and our data support their suggested protective role in IBD (Kuhl et al., 2002). $CD56^+$ αβ T cells are activated T cells and may participate in the inflammatory response.

Immunofluorescence and mass cytometry analysis revealed a tendency towards the down-regulation of the NKG2D receptor on lymphocytes in inflamed CD tissue compared to non-inflamed CD tissue and normal controls. Down-regulation of NKG2D protein was not due to a decrease in NKG2D mRNA levels in CD patients versus normal controls. We suspect that this lower NKG2D expression in inflamed tissue likely results from increased ligand expression in the inflamed mucosal gut tissue, causing ligand-induced down-regulation of NKG2D (Jimenez-Perez et al., 2012; Lundholm et al., 2014; Mincheva-Nilsson and Baranov, 2014). This contention is supported by our mass cytometry data, which showed that a higher frequency of $MICA^+$ $CD4^+$ T cells and B cells in inflamed CD samples compared with in non-inflamed CD samples and peripheral blood. In addition, a higher frequency of $MICA^+$ cells was observed in $CD45^-$ (resident tissue) cells from inflamed CD samples. HLA-DR expression on intestinal epithelial cells from CD patients has been associated with proximity to activated lymphocytes (Fais et al., 1987). Notably, we observed a higher frequency of $MICA^+$ $CD45^-$ $HLA\text{-}DR^+$ cells than $CD45^-$ $HLA\text{-}DR^-$ cells in the CD samples, suggesting that MICA expression is selectively restricted to tissue cells that co-localize with $NKG2D^+$ lymphocytes. NKG2D ligands have previously been found on epithelium, endothelium, and monocytes in CD patient (Allez et al., 2007; Glas et al., 2001; La Scaleia et al., 2012). By immunohistochemistry, we observed MICA/B expression in lymphoid aggregates, granulomas, and microvascular endothelium-like cells in CD intestines but not in healthy intestines. Moreover, germinal centers of isolated lymphoid follicles, nerve fibers, and plexuses expressed MICA/B in both CD patients and normal controls. Limited information is available regarding the expression pattern of the ULBPs in CD patients, and only ULBP1/2 expression on monocytes has previously been reported (La Scaleia et al., 2012). In this study, we document the expression pattern of all six ULBPs in CD intestine. We found that ULBP1–6, like MICA and MICB, were expressed on both immune cells and resident non-hematopoietic cells isolated from CD intestine, but that the frequencies of ligand-expressing cells were highly variable among the patients examined. The lowest expression of NKG2D ligands was observed in the two patients who received anti-TNF-α therapy approximately 3 weeks before sample collection (the normal dosing is every 8 weeks, so drug was likely present at three weeks when biopsies were taken from these patients). The mRNA levels of ULBP1, 2, and 5 support an upregulation in CD.

NKG2D ligand expression on cells can activate $NKG2D^+$ lymphocytes, resulting in increased killing of the ligand-expressing cells and/or production of cytokines, such as IFN-γ, TNF-α, and GM-CSF (Boukouaci et al., 2013; Poggi and Zocchi, 2006; Whitman and Barber, 2015). In agreement with this, we observed a positive correlation between the frequency of NKG2D ligand-expressing cells and the release of pro-inflammatory cytokines from CD biopsies in an ex vivo assay. Moreover, expression of NKG2D ligands has been

reported to enhance migration of $CD8^+$ T cells into pancreatic islets of diabetic mice (Markiewicz et al., 2012), so we examined the functional role of NKG2D and NKG2D-ligand interaction in lymphocyte migration using primary vascular endothelial cells expressing NKG2D ligands. We found that previously activated $NKG2D^+$ $CD8^+$ T cells were able to migrate through a NKG2D-ligand expressing endothelial layer by CXCL10-guided chemotaxis. The migration was dependent on an interaction between NKG2D on the $CD8^+$ T cells and NKG2D ligands on the endothelial layer, as it was significantly inhibited by the presence of a blocking anti-NKG2D antibody. These results suggest that NKG2D ligand expression on endothelial cells may contribute to lymphocyte recruitment at mucosal sites. Tissue-specific homing involves tethering, activation, and firm adhesion steps (Hart et al., 2010), and the activation might be targeted here. Activation of intestine-derived T cells has been shown to increase their migration (Hokari et al., 1999). It is therefore possible that the NKG2D and NKG2D-ligand interaction may provide an activating signal to the $CD8^+$ T cells promoting successful migration. Administration of a blocking antibody against NKG2D has been shown to significantly increase clinical remission in CD patients (Allez et al., 2014), and our results suggest that NKG2D blockade may abrogate lymphocyte cytotoxicity and cytokine production, as well as the migration, recruitment, and retention of inflammatory cells into diseased tissue in CD. In this way, anti-NKG2D antibody may uniquely interfere with both intestinal inflammation and lymphocyte homing, the two main processes targeted by current biological therapies for CD and ulcerative colitis (Mayer et al., 2014; Villablanca et al., 2011).

In conclusion, our study describes NKG2D ligand expression on several distinct cell subsets in the inflamed intestine of CD patients using three different experimental approaches to measure protein expression. Moreover, IHC and mass cytometry analyses indicated that NKG2D ligand expression on infiltrating immune cells, as well as resident intestine cells, may be specifically induced at sites of immune cell aggregation. Notably, lymphocyte infiltration in lamina propria was associated with MICA/B expression on mucosal epithelium and microvascular endothelium, lymphocytes accumulated around $MICA/B^+$ granulomas, and, finally, lymphoid follicles with MICA/B protein expression localized exclusively to the germinal centers. Inhibition of migration of $CD8^+$ T cells could be a partial mechanism of the blocking anti-NKG2D antibody currently in clinical testing in CD.

Supplementary Material

Refer to Web version on PubMed Central for supplementary material.

Acknowledgments

Funding

This work was supported by the Biopharmaceutical Research Unit, Novo Nordisk A/S, Denmark. The study sponsor did not participate in the study design or in the collection, analysis, and interpretation of data. L.L.L. is an American Cancer Society Professor and funded by NIH grant AI066897. J.C.R. was supported in part by a grant from the Crohn's and Colitis Foundation of America (CCFA).

Thanks to the nurses and doctors at the Gastrounit, Hvidovre Hospital, Denmark, for invaluable help with patient recruitment, Jan Michel Normark at Novo Nordisk A/S, for excellent technical assistance with histology, and Jesper Kastrup, at BD Bioscience, for expert advice on flow cytometry.

Abbreviations

CD	Crohn's disease
CRP	C-reactive protein
CyTOF	Cytometry by Time of Flight
DAB	diaminobenzidine
EDTA	ethylenediaminetetraacetic acid
FACS	fluorescence-activated cell sorting
FMO	fluorescence minus one
GM-CSF	granulocyte-macrophage colony-stimulating factor
HIMEC	human intestinal microvascular endothelial cells
HRP	horse radish peroxidase
IBD	inflammatory bowel disease
IFN	interferon
IL	interleukin
LPC	lamina propria cell
LPS	lipopolysaccharide
MIC	MHC class I polypeptide-related sequence
MAIT	mucosal-associated invariant T
mRNA	messenger Ribonucleic acid
NK	natural killer
NKG2D	natural-killer group 2, member D
qPCR	quantitative polymerase chain reaction
PBMC	peripheral blood mononuclear cell
TBS	Tris-buffered saline
TNF	tumor necrosis factor
TSA	tyramide signal amplification
ULBP	UL16 binding protein

References

Allegretti YL, et al. Broad MICA/B expression in the small bowel mucosa: a link between cellular stress and celiac disease. PLoS One. 2013; 8:e73658. [PubMed: 24058482]

Allez M, et al. CD4+NKG2D+ T cells in Crohn's disease mediate inflammatory and cytotoxic responses through MICA interactions. Gastroenterology. 2007; 132:2346–2358. [PubMed: 17570210]

Allez M, et al. Mo1213 efficacy and safety of NNC0142-0002, a novel human monoclonal antibody targeting NKG2D: a randomized, double-blind, single-dose phase 2 trial in patients with Crohn's disease. Gastroenterology. 2014; 146(S-587)

Bendall SC, et al. Single-cell mass cytometry of differential immune and drug responses across a human hematopoietic continuum. Science. 2011; 332:687–696. [PubMed: 21551058]

Bilbao JR, et al. HLA-DRB1 and MICA in autoimmunity: common associated alleles in autoimmune disorders. Ann N Y Acad Sci. 2003; 1005:314–318. [PubMed: 14679082]

Binion DG, et al. Enhanced leukocyte binding by intestinal microvascular endothelial cells in inflammatory bowel disease. Gastroenterology. 1997; 112:1895–1907. [PubMed: 9178682]

Boukouaci W, et al. Soluble MICA-NKG2D interaction upregulates IFN-gamma production by activated CD3-CD56+ NK cells: potential impact on chronic graft versus host disease. Hum Immunol. 2013; 74:1536–1541. [PubMed: 23994587]

Browning TH, Trier JS. Organ culture of mucosal biopsies of human small intestine. J Clin Invest. 1969; 48:1423–1432. [PubMed: 5796354]

Burgess SJ, et al. IL-21 down-regulates NKG2D/DAP10 expression on human NK and CD8+ T cells. J Immunol. 2006; 176:1490–1497. [PubMed: 16424177]

Caillat-Zucman S. How NKG2D ligands trigger autoimmunity? Hum Immunol. 2006; 67:204–207. [PubMed: 16698443]

Carapito R, Bahram S. Genetics, genomics, and evolutionary biology of NKG2D ligands. Immunol Rev. 2015; 267:88–116. [PubMed: 26284473]

Castriconi R, et al. Transforming growth factor beta 1 inhibits expression of NKp30 and NKG2D receptors: consequences for the NK-mediated killing of dendritic cells. Proc Natl Acad Sci U S A. 2003; 100:4120–4125. [PubMed: 12646700]

Cerwenka A, Lanier LL. Ligands for natural killer cell receptors: redundancy or specificity. Immunol Rev. 2001; 181:158–169. [PubMed: 11513137]

Chalupny NJ, et al. Down-regulation of the NKG2D ligand MICA by the human cytomegalovirus glycoprotein UL142. Biochem Biophys Res Commun. 2006; 346:175–181. [PubMed: 16750166]

Champsaur M, Lanier LL. Effect of NKG2D ligand expression on host immune responses. Immunol Rev. 2010; 235:267–285. [PubMed: 20536569]

Cho WK, et al. Association of MICA alleles with autoimmune thyroid disease in Korean children. Int J Endocrinol. 2012; 2012:235680. [PubMed: 23209462]

Crane CA, et al. TGF-beta downregulates the activating receptor NKG2D on NK cells and CD8+ T cells in glioma patients. Neuro-Oncology. 2010; 12:7–13. [PubMed: 20150362]

Eagle RA, et al. Beyond stressed self: evidence for NKG2D ligand expression on healthy cells. Curr Immunol Rev. 2009; 5:22–34. [PubMed: 19626129]

Fais S, et al. HLA-DR antigens on colonic epithelial cells in inflammatory bowel disease: I. Relation to the state of activation of lamina propria lymphocytes and to the epithelial expression of other surface markers. Clin Exp Immunol. 1987; 68:605–612. [PubMed: 3308219]

Fienberg HG, et al. A platinum-based covalent viability reagent for single-cell mass cytometry. Cytometry A. 2012; 81:467–475. [PubMed: 22577098]

Finck R, et al. Normalization of mass cytometry data with bead standards. Cytometry A. 2013; 83:483–494. [PubMed: 23512433]

Glas J, et al. MICA, MICB and C1_4_1 polymorphism in Crohn's disease and ulcerative colitis. Tissue Antigens. 2001; 58:243–249. [PubMed: 11782275]

Gonzalez S, et al. Immunobiology of human NKG2D and its ligands. Curr Top Microbiol Immunol. 2006; 298:121–138. [PubMed: 16329186]

Gonzalez S, et al. NKG2D ligands: key targets of the immune response. Trends Immunol. 2008; 29:397–403. [PubMed: 18602338]

Groh V, et al. Cell stress-regulated human major histocompatibility complex class I gene expressed in gastrointestinal epithelium. Proc Natl Acad Sci U S A. 1996; 93:12445–12450. [PubMed: 8901601]

Groh V, et al. Stimulation of T cell autoreactivity by anomalous expression of NKG2D and its MIC ligands in rheumatoid arthritis. Proc Natl Acad Sci U S A. 2003; 100:9452–9457. [PubMed: 12878725]

Guerra N, et al. A selective role of NKG2D in inflammatory and autoimmune diseases. Clin Immunol. 2013; 149:432–439. [PubMed: 24211717]

Gyires K, et al. Gut inflammation: current update on pathophysiology, molecular mechanism and pharmacological treatment modalities. Curr Pharm Des. 2014; 20:1063–1081. [PubMed: 23782146]

Hart AL, et al. Homing of immune cells: role in homeostasis and intestinal inflammation. Inflamm Bowel Dis. 2010; 16:1969–1977. [PubMed: 20848507]

Hokari R, et al. Altered migration of gut-derived T lymphocytes after activation with concanavalin A. Am J Phys. 1999; 277:G763–G772.

Hue S, et al. A direct role for NKG2D/MICA interaction in villous atrophy during celiac disease. Immunity. 2004; 21:367–377. [PubMed: 15357948]

Ito Y, et al. Blockade of NKG2D signaling prevents the development of murine CD4+ T cell-mediated colitis. Am J Physiol Gastrointest Liver Physiol. 2008; 294:G199–G207. [PubMed: 17962357]

Jamieson AM, et al. The role of the NKG2D immunoreceptor in immune cell activation and natural killing. Immunity. 2002; 17:19–29. [PubMed: 12150888]

Jimenez-Perez MI, et al. Cervical cancer cell lines expressing NKG2D-ligands are able to down-modulate the NKG2D receptor on NKL cells with functional implications. BMC Immunol. 2012; 13:7. [PubMed: 22316211]

Kagnoff MF. Current concepts in mucosal immunity. III Ontogeny and function of gamma delta T cells in the intestine. Am J Phys. 1998; 274:G455–G458.

Kjellev S, et al. Inhibition of NKG2D receptor function by antibody therapy attenuates transfer-induced colitis in SCID mice. Eur J Immunol. 2007; 37:1397–1406. [PubMed: 17407193]

Ko JK, Auyeung KK. Inflammatory bowel disease: etiology, pathogenesis and current therapy. Curr Pharm Des. 2014; 20:1082–1096. [PubMed: 23782147]

Kuhl AA, et al. Role of gamma delta T cells in inflammatory bowel disease. Pathobiology. 2002; 70:150–155.

La Scaleia R, et al. NKG2D/ligand dysregulation and functional alteration of innate immunity cell populations in pediatric IBD. Inflamm Bowel Dis. 2012; 18:1910–1922. [PubMed: 22294522]

Lanier LL. NKG2D receptor and its ligands in host defense. Cancer Immunol Res. 2015; 3:575–582. [PubMed: 26041808]

Lee JC, et al. Elevated TGF-beta1 secretion and down-modulation of NKG2D underlies impaired NK cytotoxicity in cancer patients. J Immunol. 2004; 172:7335–7340. [PubMed: 15187109]

Lin D, et al. NF-kappaB regulates MICA gene transcription in endothelial cell through a genetically inhibitable control site. J Biol Chem. 2012; 287:4299–4310. [PubMed: 22170063]

Liu W, Huber SA. Cross-talk between cd1d-restricted nkt cells and gammadelta cells in t regulatory cell response. Virol J. 2011; 8:32. [PubMed: 21255407]

Lundholm M, et al. Prostate tumor-derived exosomes down-regulate NKG2D expression on natural killer cells and CD8+ T cells: mechanism of immune evasion. PLoS One. 2014; 9:e108925. [PubMed: 25268476]

Lundqvist C, et al. Isolation of functionally active intraepithelial lymphocytes and enterocytes from human small and large intestine. J Immunol Methods. 1992; 152:253–263. [PubMed: 1500733]

Maasho K, et al. NKG2D is a costimulatory receptor for human naive CD8+ T cells. J Immunol. 2005; 174:4480–4484. [PubMed: 15814668]

Markiewicz MA, et al. RAE1epsilon ligand expressed on pancreatic islets recruits NKG2D receptor-expressing cytotoxic T cells independent of T cell receptor recognition. Immunity. 2012; 36:132–141. [PubMed: 22244846]

Mayer L, et al. Anti-IP-10 antibody (BMS-936557) for ulcerative colitis: a phase II randomised study. Gut. 2014; 63:442–450. [PubMed: 23461895]

Mincheva-Nilsson L, Baranov V. Cancer exosomes and NKG2D receptor-ligand interactions: impairing NKG2D-mediated cytotoxicity and anti-tumour immune surveillance. Semin Cancer Biol. 2014; 28:24–30. [PubMed: 24602822]

Muntasell A, et al. Inhibition of NKG2D expression in NK cells by cytokines secreted in response to human cytomegalovirus infection. Blood. 2010; 115:5170–5179. [PubMed: 20393128]

O'Callaghan CA, et al. Molecular competition for NKG2D: H60 and RAE1 compete unequally for NKG2D with dominance of H60. Immunity. 2001; 15:201–211. [PubMed: 11520456]

Orchard TR, et al. MHC class I chain-like gene A (MICA) and its associations with inflammatory bowel disease and peripheral arthropathy. Clin Exp Immunol. 2001; 126:437–440. [PubMed: 11737059]

Park YP, et al. Complex regulation of human NKG2D-DAP10 cell surface expression: opposing roles of the gammac cytokines and TGF-beta1. Blood. 2011; 118:3019–3027. [PubMed: 21816829]

Poggi A, Zocchi MR. Antigen presenting cells and stromal cells trigger human natural killer lymphocytes to autoreactivity: evidence for the involvement of natural cytotoxicity receptors (NCR) and NKG2D. Clin Dev Immunol. 2006; 13:325–336. [PubMed: 17162374]

Radulovic K, Niess JH. CD69 is the crucial regulator of intestinal inflammation: a new target molecule for IBD treatment? J Immunol Res. 2015; 2015:497056. [PubMed: 25759842]

Raulet DH, et al. Regulation of ligands for the NKG2D activating receptor. Annu Rev Immunol. 2013; 31:413–441. [PubMed: 23298206]

Rieder F, et al. Inflammation-induced endothelial-to-mesenchymal transition: a novel mechanism of intestinal fibrosis. Am J Pathol. 2011; 179:2660–2673. [PubMed: 21945322]

Roberts AI, et al. NKG2D receptors induced by IL-15 costimulate CD28-negative effector CTL in the tissue microenvironment. J Immunol. 2001; 167:5527–5530. [PubMed: 11698420]

Schrambach S, et al. In vivo expression pattern of MICA and MICB and its relevance to auto-immunity and cancer. PLoS One. 2007; 2:e518. [PubMed: 17565371]

Shacklett BL, et al. Optimization of methods to assess human mucosal T-cell responses to HIV infection. J Immunol Methods. 2003; 279:17–31. [PubMed: 12969544]

Tsilingiri K, et al. Probiotic and postbiotic activity in health and disease: comparison on a novel polarised ex-vivo organ culture model. Gut. 2012; 61:1007–1015. [PubMed: 22301383]

Upshaw JL, Leibson PJ. NKG2D-mediated activation of cytotoxic lymphocytes: unique signaling pathways and distinct functional outcomes. Semin Immunol. 2006; 18:167–175. [PubMed: 16723257]

Villablanca EJ, et al. Blocking lymphocyte localization to the gastrointestinal mucosa as a therapeutic strategy for inflammatory bowel diseases. Gastroenterology. 2011; 140:1776–1784. [PubMed: 21530744]

Whitman E, Barber A. NKG2D receptor activation of NF-kappaB enhances inflammatory cytokine production in murine effector CD8(+) T cells. Mol Immunol. 2015; 63:268–278. [PubMed: 25089028]

Zhang C, et al. Interleukin-12 improves cytotoxicity of natural killer cells via upregulated expression of NKG2D. Hum Immunol. 2008; 69:490–500. [PubMed: 18619507]

Appendix A. Supplementary data

Supplementary data to this article can be found online at http://dx.doi.org/10.1016/j.yexmp.2017.06.010.

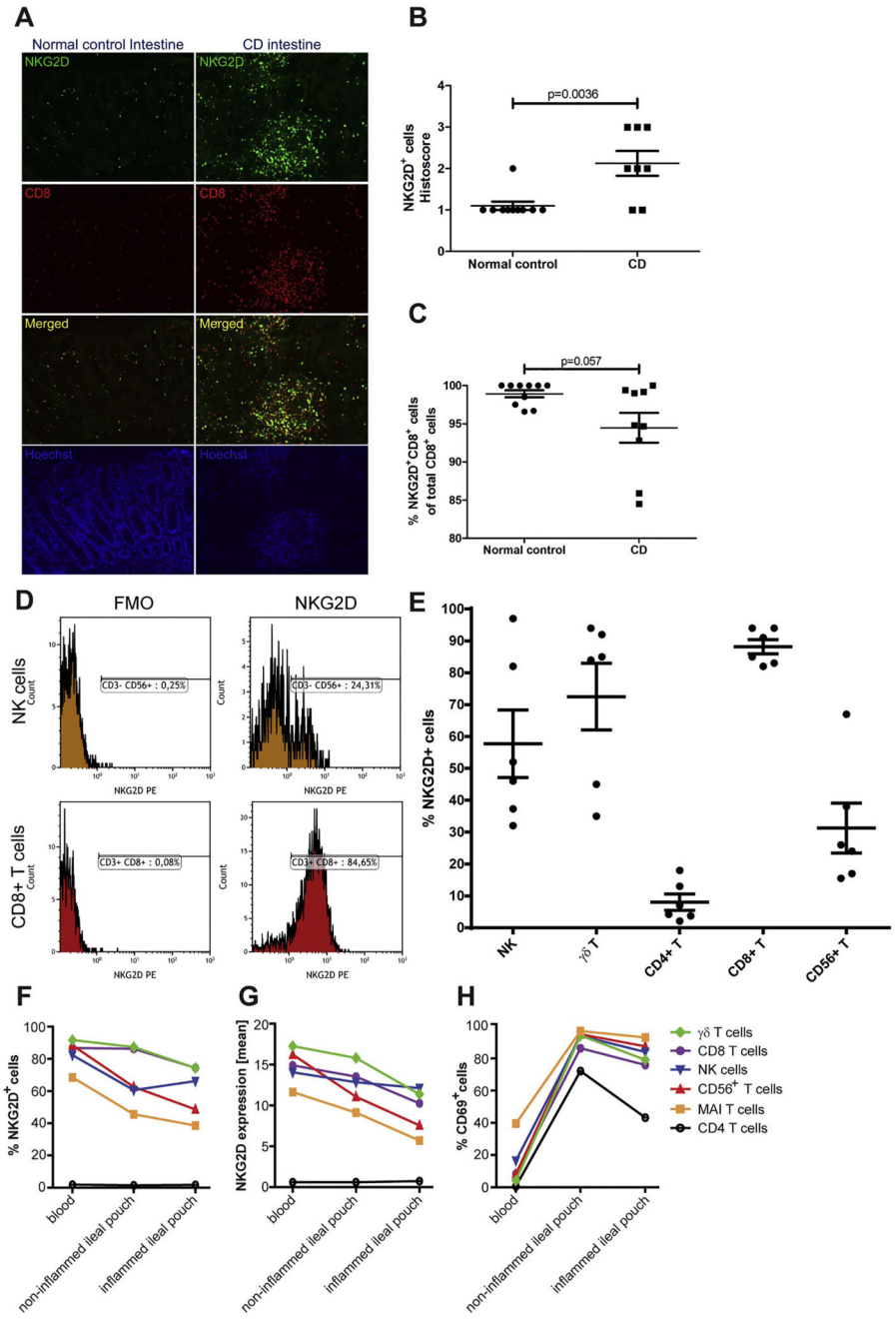

Fig. 1.

NKG2D expression decreases in inflamed tissue and is diverse on different cell subtypes. (A) Immunofluorescence staining of NKG2D (green), CD8 (red), and nuclei (blue) on mucosa of normal control colon (left panel) and inflamed CD colon (right panel). (B) Semi-quantitative scoring (range: 1–3) of number of $NKG2D^+$ cells on $NKG2D^+$ and $CD8^+$ immunofluorescence-stained tissue sections in normal control (n = 10) and CD (n = 11) intestinal samples. *t*-Test with mean ± SEM. (C) Quantitative analysis of NKG2D and CD8 immunofluorescence-stained tissue sections of normal control (n = 10) and CD (n = 9) intestinal samples. *t*-Test with mean ± SEM. (D) Representative histograms of flow

cytometry NKG2D expression gating on NK cells and $CD8^+$ T cells. Gates were set on live cells with a forward angle and side scatter profile containing lymphocytes and then further gated on $CD45^+CD3^-$ $\gamma\delta TCR^-CD56^+$ NK cells and $CD45^+CD56^-CD3^+CD8^+$ T cells from the same patient. (E) Flow cytometry analysis of NKG2D expression on specific lymphocyte subsets in the colon of six inflamed CD patients. Shown with mean ± SEM. (F–H) Lymphocytes isolated from peripheral blood and intestine biopsies obtained from CD patients. Percentages of cells expressing NKG2D (F), mean NKG2D expression (G), and percentages of cells expressing CD69 (H) were examined on the indicated lymphocyte populations by mass cytometry. Graphs show data from CD patient #1. A similar trend was observed for CD patient #2. (For interpretation of the references to color in this figure legend, the reader is referred to the web version of this article.)

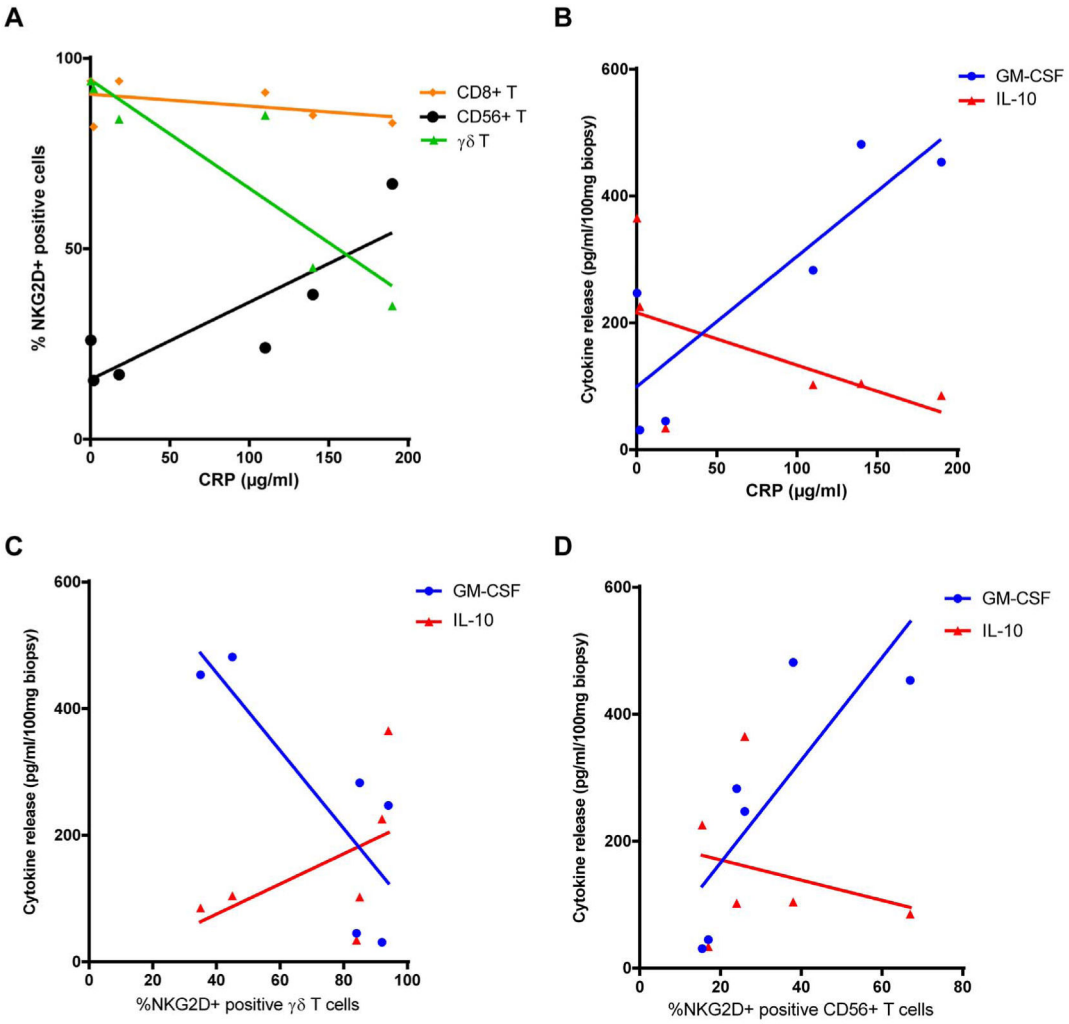

Fig. 2.

Frequency of T cell subtypes expressing NKG2D correlates with CRP levels. (A) Serum CRP amounts in CD patients correlated with the percentages of NKG2D-expressing cell types. The linear regression is significantly non-zero for $CD56^+$ T cells ($CD45^+CD3^+$ $\gamma\delta TCR^-CD56^+$) and γδ T cells ($CD45^+CD3^+$ $\gamma\delta TCR^+$) ($P = 0.0311$ and 0.01470.05, $R^2 = 0.7266$ and 0.8085, respectively). $CD4^+$ T and NK cells show similar results to $CD8^+$ T cells ($R^2 = 0.3611$), $P > 0.05$ for all. (B) Linear regression of CRP amounts vs. cytokine release from biopsies in explant culture from the same patients. The significantly positive correlation of GM-CSF ($P = 0.0267$, $R^2 = 0.7457$) is shown (IL-1β, INF-γ and TNF-α showed the same tendency) along with the negative correlation tendency of IL-10 ($P = 0.2580$, $R^2 = 0.3027$). Percentage of γδ T cells (C) and $CD56^+$ T cells (D) expressing NKG2D vs. cytokine release show opposite trends (IL-1β, INF-γ and TNF-α showed the same tendency as GM-CSF, which has $P = 0.0458$, $R^2 = 0.6721$ in C and $P = 0.0422$, $R^2 = 0.6514$ in D). IL-10 has $P = 0.3085$, $R^2 = 0.2535$ in C and $P = 0.6303$, $R^2 = 0.0634$ in D. n = 6 patients, 4 biopsies each.

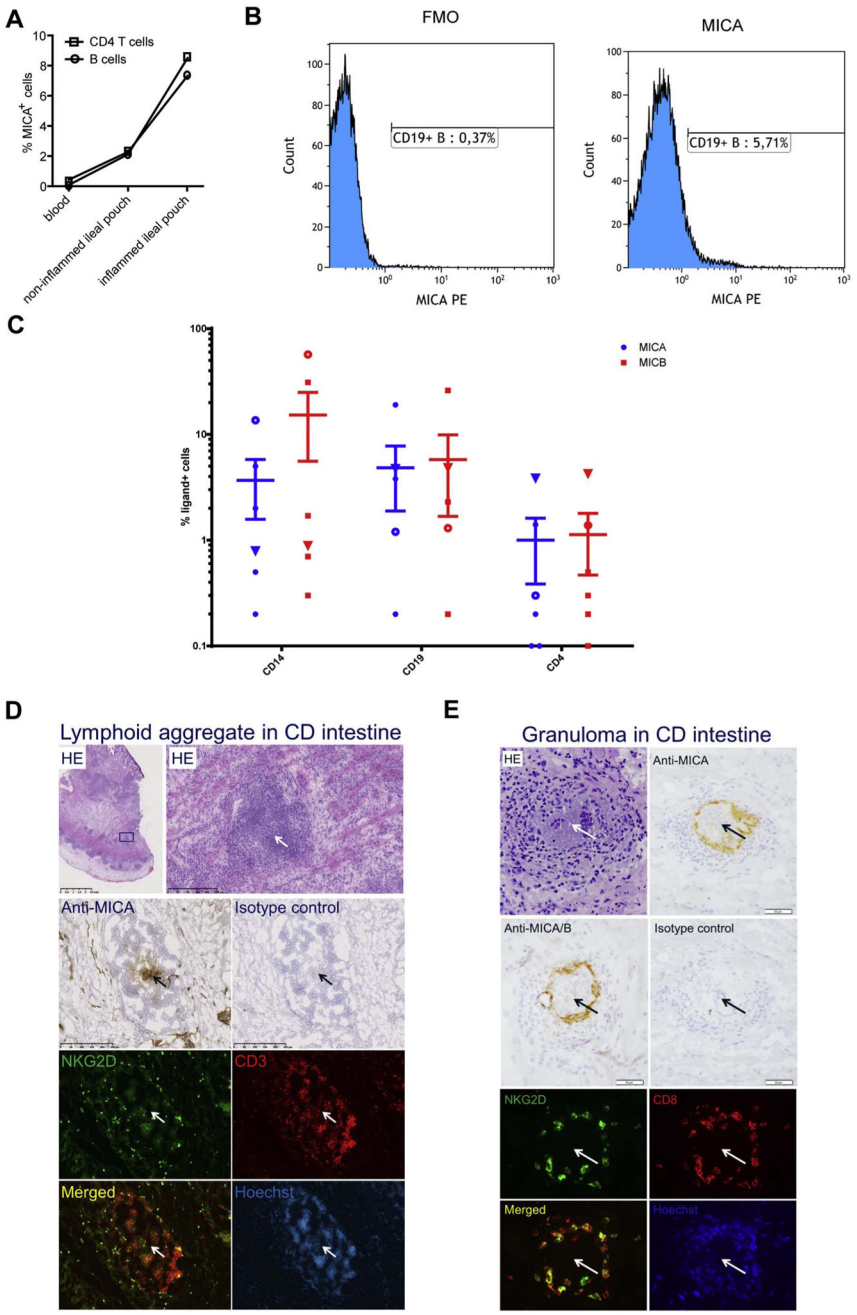

Fig. 3.

MICA and MICB expression by immune cells in CD intestine. (A) Frequencies of $CD4^+$ T and $CD19^+$ B cells expressing MICA in blood and non-inflamed and inflamed biopsies as detected by mass cytometry. Graphs show data from CD patient #1. A similar trend was observed for CD patient #2. (B) Representative histograms of MICA expression on $CD45^+CD3^-CD19^+$ B cells, pre-gated on live lymphocytes. (C) Frequency of cells expressing MICA and MICB in intestine from six inflamed CD patients on $CD14^+$ myeloid cells, $CD19^+$ T cells, and $CD4^+$ T cells as measured by flow cytometry. Open dots and triangles denote data points from the same patients across cell types (mean ± SEM, Y-axis is

log10). (D) Anti-MICA IHC staining in lymphoid aggregates with $NKG2D^+$ cells. Upper panel shows low and high power images of HE-stained inflamed CD intestine (box in low-power image indicates lymphoid aggregate depicted in the high-power image). Serial sections were immunostained with anti-MICA and isotype-matched control antibodies as indicated or subjected to immunofluorescence for detection of NKG2D (green fluorescence). Co-staining for $CD3^+$ cells (red fluorescence) and nuclei counterstaining (Hoechst) were used to visualize the localization of $NKG2D^+$ cells in the lymphoid aggregate. Arrows indicates the localization of $MICA^+$ cells in the center of the lymphoid aggregate. A similar staining pattern was observed with anti-MICA/B antibody (not shown). Size of scale bars are indicated in the images. (E) Upper two panels show IHC staining with anti-MICA (AMO1), anti-MICA/B (AMO1) and isotype-matched control IgG1 antibodies and HE staining of serial sections of CD intestine. Lower two panels show immunofluorescence co-staining of NKG2D (green), CD8 (red), and nuclei (blue) on serial sections of the same CD intestine. Images show accumulation of cells expressing NKG2D and MICA/B positive cells in a granuloma in inflamed CD intestine. Arrows indicate the central epithelioid macrophages of the granuloma. The size of scale bars is indicated in the images. (For interpretation of the references to color in this figure legend, the reader is referred to the web version of this article.)

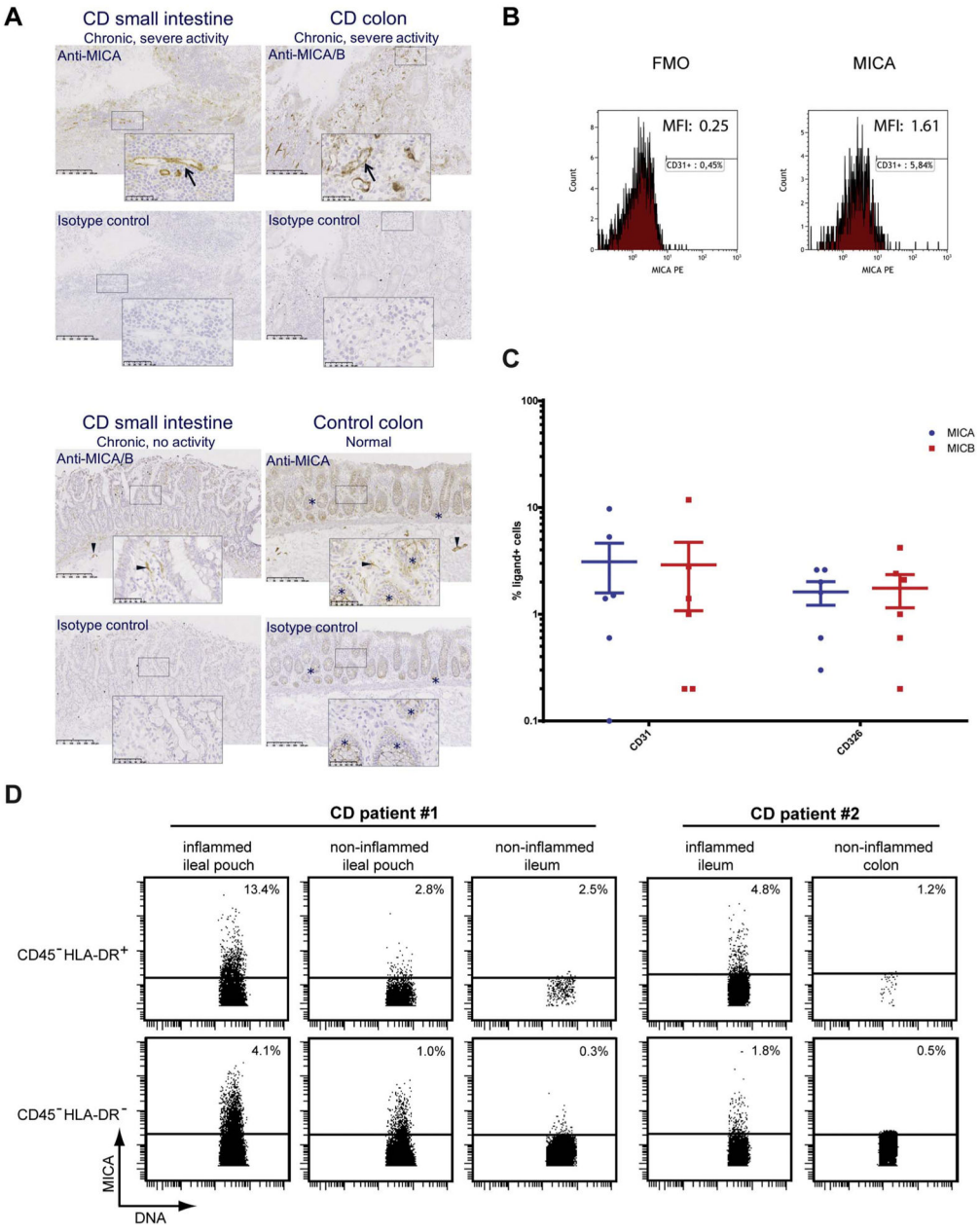

Fig. 4.

Expression of MICA and MICB by non-hematopoietic cells in CD and normal control. (A) Immunohistochemistry with anti-MICA/B antibody (BAMO1), anti-MICA antibody (AMO1), or an isotype-matched control IgG1 on CD small intestine and colon with chronic inflammation and severe activity (upper panels), CD small intestine with chronic inflammation and no activity (lower left panel), and normal control colon (lower right panel). Boxes indicate area of the images that are depicted in the high-power images. Arrows in the upper panels indicate anti-MICA and anti-MICA/B immunostained microvascular endothelial-like cells. Arrowheads in the lower panels indicate anti-MICA and anti-MICA/B immunostained nerve fiber- and submucous plexus-like structures. Asterisks

indicate non-specific staining of mucosal epithelium. Size of scale bars is indicated in the images. (B) Representative flow cytometry histograms of MICA expression with geometric MFI values: $CD45^{-}CD31^{+}$ endothelial cells in the non-hematopoietic population, pre-gated on live cells. FMO includes isotype-matched control staining. (C) Flow cytometry analysis of MICA and MICB expression on $CD31^{+}$ endothelial and $CD326^{+}$ epithelial cells in gut from six inflamed CD patients (mean ± SEM, Y-axis is log10). (D) Mass cytometry analysis of MICA expression on $CD45^{-}HLA\text{-}DR^{+}$ cells (i.e. non-hematopoietic tissue cells adjacent to lymphoid tissue) and $CD45^{-}HLA\text{-}DR^{-}$cells (i.e. tissue cells not adjacent to lymphoid tissue). Data from CD patient #1 and #2.

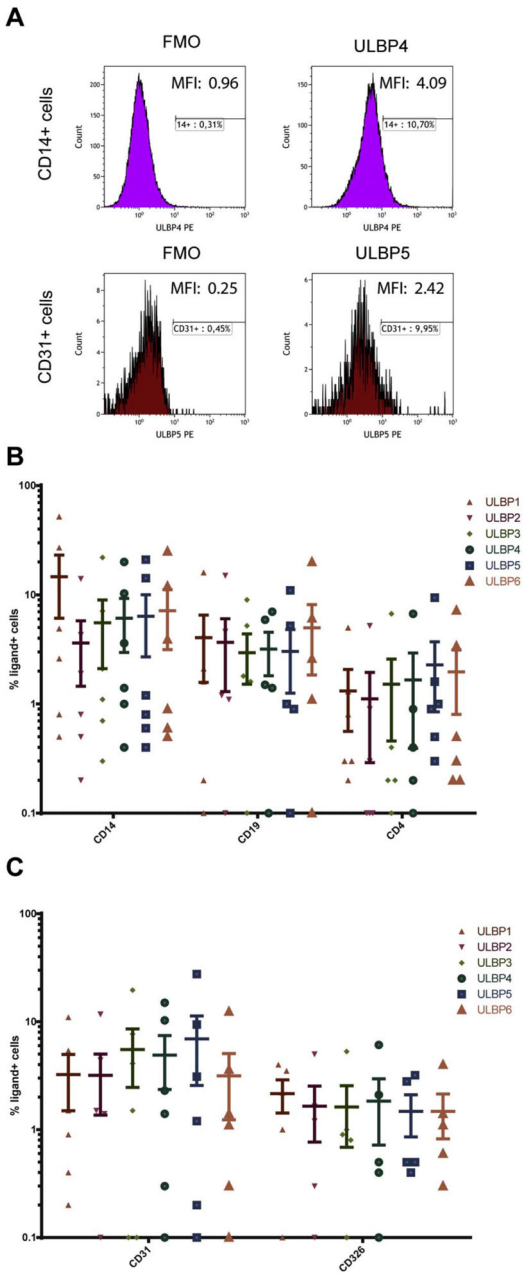

Fig. 5.

Expression patterns of ULBP1–6 in inflamed CD intestine. (A) Representative flow cytometry histograms with geometric MFI values of ULBP4 expression on viable $CD45^{+}$lymphocyte$^{-}CD14^{+}$ myeloid cells and ULBP5 on $CD45^{-}CD31^{+}$endothelial cells. Flow cytometry analysis of ULBP1–6 expression in intestine from six inflamed CD patients on $CD14^{+}$, $CD19^{+}$, and $CD4^{+}$ immune cells (B) and $CD31^{+}$ endothelial and $CD326^{+}$ epithelial cells (C) (mean ± SEM, Y-axis is log10).

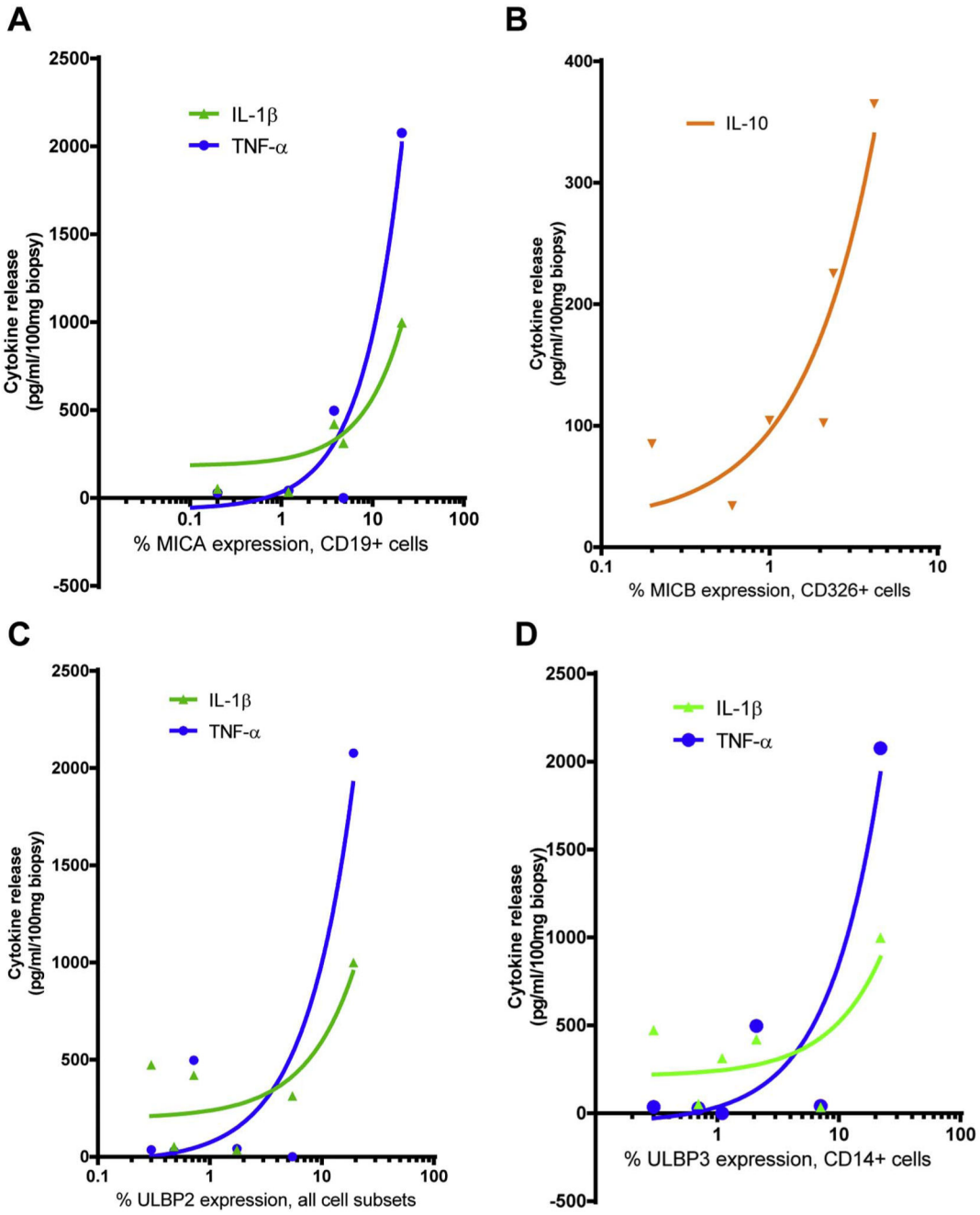

Fig. 6.

Correlation of expression patterns of MICA, MICB, and ULBP1–6 in inflamed CD intestine with cytokine release. Percentages of $CD19^+$ B cells expressing MICA (A) and $CD326^+$ epithelial cells expressing MICB (B) vs. cytokine release (R^2 for IL-1β = 0.75, for TNF-α = 0.93, for IL-10 = 0.85). (C) Percentages of all cell subsets ($CD4^+$ T, $CD19^+$ B, $CD326^+$ epithelial, $CD31^+$ endothelial cells, and $CD14^+$ myeloid cells) expressing ULBP2 vs. cytokine release (R^2 for IL-1β = 0.68, for TNF-α = 0.85). (D) Percentages of $CD14^+$ myeloid cells expressing ULBP3 vs. cytokine release (R^2 for IL-1β = 0.73, for TNF-α =

0.86). All linear regression lines shown are non-zero with $P < 0.05$ and n = 6 patients, 4 biopsies each. X-axis is log10. The regression findings for each cell type are representative for the majority or all of ligands.

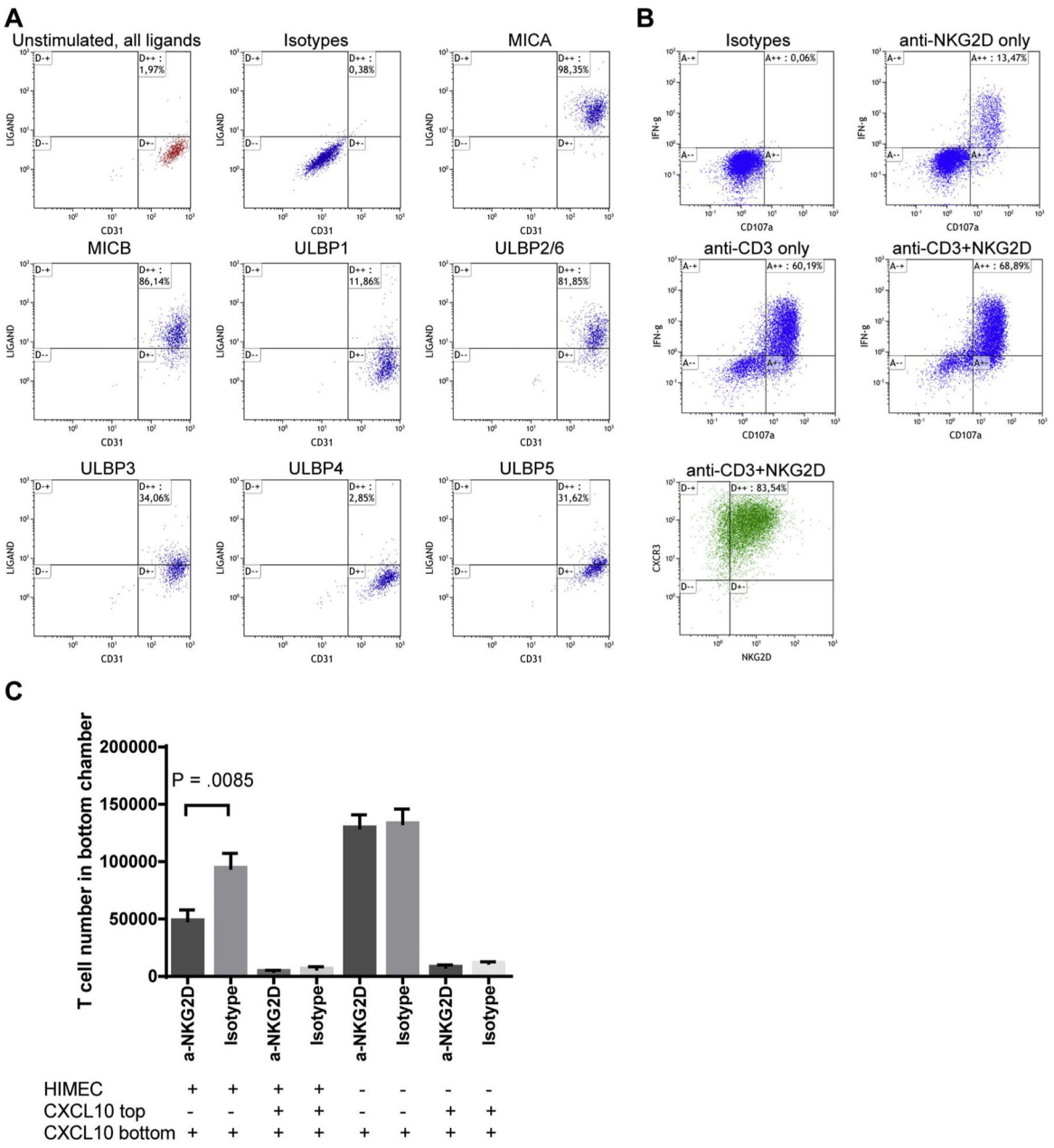

Fig. 7.

Blocking anti-NKG2D antibody inhibits in vitro migration of activated $CD8^+$ T cells across microvascular endothelial cells expressing NKG2D ligands. (A) Flow cytometry plots of IFN-α (100 U/ml) and LPS (1 μg/ml)-stimulated (10 h) healthy human intestinal microvascular endothelial cells (HIMEC) analyzed for NKG2D ligands. All ligands on unstimulated cells are shown in the upper left corner (red color) followed by the isotype-matched Ig controls and the individual ligands as indicated on stimulated cells. (B) $CD8^+$ T cells were stimulated with anti-CD3 and IL-2 for three days and then cultured in IL-2 for 9 days to prime NKG2D-responsiveness. The pre-activated T cells were then re-stimulated for 4 h with plate-bound isotype-matched control IgG1, anti-NKG2D, anti-CD3, and both anti-

CD3 + anti-NKG2D. Flow cytometry analysis of CD107a (degranulation marker) and IFN-γ, with insert (green color) showing expression of CXCR3 and NKG2D on the stimulated T cells. (C) Transwell assay to determine cell migration in response to CXCL10 of activated $CD8^+$ T cells with and without blocking anti-NKG2D over an HLIMEC layer. 100 ng/ml of CXCL10 chemokine was included in the medium of the bottom chamber to induce chemotaxis or in both chambers as a control (n = 12 transwells from 2 blood donors, $P = 0.0085$, *t*-test, mean ± SEM). (For interpretation of the references to color in this figure legend, the reader is referred to the web version of this article.)

Table 1

Expression % of NKG2D ligands on human intestinal microvascular endothelial cells with or without LPS and IFN-α stimulation.

Ligand	HIMEC (% cells positive for ligand expression)		HLIMEC (% cells positive for ligand expression)	
	Unstimulated	Stimulated	Unstimulated	Stimulated
MICA	0	98	99	99
MICB	0	86	95	98
ULBP1	0	12	30	48
ULBP2/6	0	82	98	97
ULBP3	0	34	90	95
ULBP4	0	3	29	32
ULBP5	0	32	23	30